Experimental Study of the Impact of Boundary Conditions on Oil Recovery by Co-Current and Counter-Current Spontaneous Imbibition

Dag Chun Standnes*

Centre for Integrated Petroleum Research (CIPR), University of Bergen, Allégaten 41, N-5007 Bergen, Norway

Received July 18, 2003. Revised Manuscript Received October 14, 2003

Spontaneous imbibition (SI) is a very important oil recovery mechanism from low-permeability fractured reservoirs. The impact of different sample shapes and boundary conditions on oil recovery by counter-current and co-current SI into low-permeability (≈2 mD) strongly water-wet outcrop chalk have been investigated. The experimental program was divided into two parts. In part 1, counter-current SI was studied by submerging cubic, cylindrical, and irregular rock samples totally in the aqueous phase, whereas co-current SI was investigated in part 2 by exposing different portions of a cubic rock sample to an oil-phase. The scaling law of Ma et al.[1] was used to correlate counter-current SI data with all parameters than the characteristic length, L_C, held essentially constant. The results confirm the ability for L_C to account for cylindrical (diameters in the range from ≈2 to 10 cm) and cubic sample shapes and different no-flow surface boundary conditions (2, 4 and 5 faces were coated with polyester on the cubic rock samples; top and bottom faces on the cylindrical cores). Rock samples having irregular shapes (increasing and decreasing cross-sectional areas were investigated) could not be scaled according to L_C because the overall shape of the imbibition curves deviated from curves generated by rock samples having regular shape. No scaling law correlating imbibition data for different boundary conditions exists for tests performed under co-current flow conditions; hence the results in part 2 of the experimental program are interpreted qualitatively. When using the SI rate for a cube with all faces open to imbibition as the reference (counter-current flow conditions), the results show that depending on the area fraction of the cube covered by oil, co-current SI can either be faster (water−oil area-ratio (WOAR) > 1), equal (WOAR = 1) or slower (WOAR < 1)) than the reference system. In all cases, ultimate recovery is significantly higher for tests performed under co-current flow conditions than under counter-current (70% of initially oil in place (IOIP) vs 58% IOIP for counter-current). The results indicate that when evaluating oil recovery potential on reservoir rock samples due to SI experimentally, tests should be performed both under co-current and counter-current flow conditions because the latter one might under certain circumstances predict too low rates and ultimate recoveries.

Introduction

The process when fluids are sucked into a porous medium by the action of capillary forces is referred to as spontaneous imbibition (SI). SI of water into the matrix blocks is regarded as a very important driving mechanism for oil recovery in fractured water-wet reservoirs. The process is very complex and depends on numerous parameters such as wettability of the porous medium, shape, size, boundary conditions, and permeability of the rock material in addition to fluid properties such as viscosities and oil−water interfacial tension (IFT). The effects of different sample shapes, sizes, and boundary conditions on the SI process are the subject in this work.

Depending on the fluid distribution around the rock sample (matrix block) during the imbibition process, two modes of SI referred to as counter-current and co-current imbibition may take place. Counter-current SI occurs when the rock sample is totally submerged in water (counter-current flow still apply even if some portion of the rock surface is covered by an impermeable coating referred to here as no-flow surface (NFS)). In this case, oil is flowing in the opposite direction of water and produced from the same surfaces water entered the porous medium. Co-current flow of oil and water may occur when a portion of the rock sample is in contact with oil during the imbibition process. Oil and water can then flow in the same direction in the porous medium because oil can be produced from parts of the rock surface covered by this phase.

Counter-current SI has been regarded as the most important driving mechanism of the two modes, which is reflected in the numerous numbers of experimental and numerical papers treating this subject. Further references can be obtained from a recent review of the state of the art by Morrow and Mason.[2]

* Corresponding author. Tel: +47 55 58 33 74. Fax: +47 55 58 82 65. E-mail: dag.standnes@cipr.uib.no.

(1) Ma, S.; Zhang, X.; Morrow, N. R. *CIM paper* **1995**, No. 95-94.

10.1021/ef030142p CCC: $27.50
Published on Web 12/11/2003

Torsæter and Silseth[3] performed an extensive qualitative investigation of the effects of boundary conditions and sample shape on oil recovery by capillary imbibition (counter-current flow in almost all tests). They concluded that oil recovery rate increased with increasing area-to-volume ratio of the rock sample. However, to correlate SI behavior for rocks having different properties and to draw general conclusions about the imbibition process, it is necessary to introduce so-called scaling laws where oil recovery from a given rock sample is expressed as a function of dimensionless time. Based on the work of Rapoport,[4] the first published scaling law describing SI in rock−water−oil systems was published by Mattax and Kyte[5] in 1962. Their classical scaling law reads as follows:

$$t_{D,MK} = \sqrt{\frac{k}{\phi}} \cdot \frac{\sigma}{\mu_w} \cdot \frac{1}{L_{C,MK}^2} \cdot t \qquad (1)$$

where $t_{D,MK}$ represents dimensionless time (−) (Mattax-Kyte), k is absolute permeability (m^2), $L_{C,MK}$ is characteristic length (m); μ_w is water viscosity (Pa·s), Φ is porosity (fraction), t is imbibition time (s), and σ is oil−water IFT (N/m).

This scaling law is valid under the assumptions of similar rock sample shape, fluid viscosities, initial fluid distribution, and relative permeability and capillary pressure functions between matrix block and laboratory model. In addition, gravity effects should be negligible. Knowing oil recovery vs time for a system with known rock-fluid properties (k, σ, μ_w, Φ, and $L_{C,MK}$), oil recovery vs time can be predicted for other systems having different values of k, σ, μ_w, Φ, and $L_{C,MK}$ because equal dimensionless times should give the same oil recovery when plotting oil recovery as a percentage of recoverable oil vs $t_{D,MK}$. The characteristic length term, $L_{C,MK}$, not specified further by Mattax and Kyte has been generalized to account for different sample shapes and NFS boundary conditions. For a rock sample with n surfaces available for counter-current water imbibition, Zhang et al.[6] expressed the characteristic length named L_C as follows:

$$L_C^2 = \frac{V_b}{\sum_{i=1}^{n} \frac{A_i}{l_i}} \qquad (2)$$

where V_b represents bulk volume of the rock sample (m^3), A_i is the area of the ith imbibition surface (m^2), and l_i is the distance from the ith imbibition surface to the no-flow boundary (NFB) (m).

Equation 2 has been shown to account for a wide range of different sample sizes and boundary conditions based on previously published counter-current SI data.[5,7,8] Substituting eq 2 into eq 1 gives a generalized scaling law for counter-current SI according to Ma et al.:[1]

$$t_{D,MZM} = \sqrt{\frac{k}{\phi}} \cdot \frac{\sigma}{\mu_g} \cdot \frac{1}{L_C^2} \cdot t = C \cdot \frac{1}{L_C^2} \cdot t \qquad (3)$$

where $C = \sqrt{k/\phi} \cdot \sigma/\mu_g$); $t_{D,MZM}$ is dimensionless time (Ma-Zhang-Morrow); and μ_g is the geometric mean of oil and water viscosities. The numerical value of $C = 3.2 \times 10^{-6}$ m^2/s (using typical values of the applied rock−fluid system: $k = 2 \times 10^{-15}$ m^2, $\Phi = 0.42$, $\sigma = 0.046$ N/m, $\mu_g = 1 \times 10^{-3}$ Pa·s), and other parameters as defined above.

As mentioned above, co-current SI has received much less attention than counter-current SI. Nevertheless, the condition for co-current flow to occur (some portion of the rock sample is covered by oil instead of water) is very often fulfilled in the reservoir when oil and water are segregating in the fracture system. Pooladi-Darvish and Firoozabadi[9] showed that Rapoport's general scaling law also applies for 1-D co-current flow of oil and water varying the permeability, capillary pressure, viscosity of the oil phase, and the length of the core sample. However, no L_C expression like eq 2 accounting for boundary conditions such as NFS and different oil coverage on the rock sample exists for tests performed under co-current flow conditions. Consequently, the results for this flow mode must be interpreted qualitatively.

Several authors have shown qualitatively that boundary conditions allowing co-current flow can have major impacts on the oil recovery rate. Bourbiaux and Kalaydjian[10] performed SI on a laterally coated sandstone sample, and they observed faster and higher oil recovery when exposing the top surface of the rock sample to an oil phase (co-current flow conditions) compared to the case where both top and bottom were exposed to brine (counter-current flow). They concluded that co-current flow is faster than counter-current. Pooladi-Darvish and Firoozabadi[9,11] performed experimental and numerical work on stacks of matrix blocks of Berea and Kansas chalk that experience a rising fracture water level. Tests were also conducted on rock samples totally immersed in water for comparison, and their work also indicated that co-current flow can be faster and ultimate recovery higher than for counter-current flow. The objectives of this work are the following:

(i) Quantitative testing of the L_C term in eq 3 for an extended collection of rock sample shapes, sizes, and boundary conditions (part 1 in the experimental program). Counter-current SI tests were performed on cylindrical, cubic, and irregular chalk samples (mimicking the reservoir rock in the chalk fields in the North Sea) of low permeability (≈2 mD) having either all faces open to imbibition or some surfaces coated with polyester. Since all parameters included in C in eq 3 are essentially constant, oil recovery vs $t_{D,MZM}$ depends only on L_C.

(ii) Investigate oil recovery rates due to co-current flow of oil and water as compared to counter-current

(2) Morrow, N. R.; Mason, G. *Curr. Opin. Colloid Interface Sci* **2001**, *6*, 321−337.
(3) Torsæter, O.; Silseth, J. K. *Paper 10 presented at the Norwegian Petroleum Directorate/Danish Energy Agency Chalk research program Symposium/Seminar*; Stavanger, Norway, May 21−22, 1985.
(4) Rapoport, L. A. *Pet. Trans., AIME* **1955**, *204*, 143−150.
(5) Mattax, C. C.; Kyte, J. R. *SPE J.* **1962**, *June*, 177−184.
(6) Zhang, X.; Morrow, N. R.; Ma, S. *SPE paper* **1995**, No. 30762.
(7) Hamon, G.; Vidal, J. *SPE paper* **1986**, No. 15852.
(8) Ma, S.; Morrow, N. R.; Zhang, X. *J. Pet. Sci. Eng.* **1997**, *18*, 165−178.
(9) Pooladi-Darvish, M.; Firoozabadi, A. *SPE J.* **2000**, *5* (1), 3−11.
(10) Bourbiaux, B. J.; Kalaydjian, F. *J. SPERE* **1990**, *August*, 361−368.
(11) Pooladi-Darvish, M.; Firoozabadi, A. *CIM paper* **1998**, No. 98-55.

Table 1. Fluid Properties

liquid phase	density at 20 °C (g/cm^3)	viscosity at 20 °C (mPa·s)	IFT using decane as oil phase at 20 °C (mN/m)
distilled water	0.9982	1.0	46
n-decane	0.731	0.95	–

Table 2. Core Data from SI Tests Performed in Part 1 of the Experimental Program Varying Rock Sample Shape and Boundary Conditions

test no.	sample shape-boundary condition	$V_b \times 10^{-6}$ (m^3)	PV $\times 10^{-6}$ (m^3)	porosity (%)	# flow dimensions
1	CY-AFO	43.10	17.98	41.7	3-D
2	CY-AFO (repeated test 1)	43.10	18.57	43.1	3-D
3	CY-2FC	15.55	6.68	43.0	2-D
4	CY-2FC	44.77	19.06	42.6	2-D
5	CY-2FC	90.48	38.36	42.4	2-D
6	CY-2FC	311.8	134.7	43.2	2-D
7	CU-AFO	54.29	22.97	42.3	3-D
8	CU-2FC	54.44	23.60	43.4	3-D
9	CU-2FC (repeated test 8)	54.44	23.54	43.2	3-D
10	CU-4FC	54.48	24.05	44.1	2-D
11	CU-4FC(S) (symmetric)	54.87	23.59	43.0	1-D
12	CU-5FC	54.72	23.91	43.7	1-D
13	IR-DCA	54.70	23.03	42.1	1-D
14	IR−CCA	54.30	23.60	43.5	1-D
15	IR−ICA	47.90	20.48	42.8	1-D

(part 2 of the experimental program). Co-current SI tests were performed on a cube of low-permeability chalk (referred to as a unit matrix block (UMB)) varying the fraction of the surface covered by oil. The UMB was also coated with polyester (NFS) in some of the tests for the sake of comparison.

Experimental Section

Fluids. *n*-Decane from Riedel-deHäen with grade >95% was used as oil phase. This model oil will not modify the wettability of the porous medium which is confirmed through excellent reproducibility. The density of the oil phase was 0.731 g/cm^3 at 20 °C. Distilled water was used as the imbibing water phase. Fluid properties for the SI tests are summarized in Table 1.

Porous Medium. Outcrop chalk samples from Denmark were used as porous medium. The samples were taken from the same block and porosities were all close to 42% and absolute permeability was determined to be approximately 2 mD. This type of chalk has been used previously as a model porous medium mimicking the matrix block properties of the chalk fields in the North Sea. Different NFS boundary conditions were obtained by coating imbibition surfaces with Glasfiberspackel (polyester) from Hagmans Kemi AB Sweden to the desired boundary condition. Rock properties for all tests are shown in Tables 2 and 3.

***n*-Decane−Water IFT.** *n*-Decane−water IFT was determined to 46 mN/m at ambient temperature using a ring-tensiometer.

Rock Sample Geometries. The different geometries and boundary conditions investigated are described in Figures 1, 2, 3 and 4. Rock samples having cubic, cylindrical, or irregular shapes/boundary condition are called CU, CY, and IR, respectively, whereas boundary conditions are referred to as AFO (all face open), 1 FC (1 face coated), 2 FC (2 faces coated), etc. General expressions for L_C for the different geometries/boundary conditions in part 1 of the experimental program are given in Table 4. Part 2 of the experimental program include several tests on a 5.0 × 5.0 × 5.0 cm^3 cube (UMB), and rock sample data and boundary conditions used in these tests are provided in Table 3.

Spontaneous Imbibition Tests. All SI tests were performed at ambient temperature (≈20 °C). The tests in part 1 of the experimental program were performed using Amott cells except the tests performed on the cylindrical cores with diameter 6.00 and 10.00 cm. Tests in the Amott cells were performed by introducing 100% oil-saturated cores into the cell, adding distilled water, and monitoring oil production as a function of time. The oil production could be measured with an accuracy of ±0.1 mL. In case of the cylindrical cores having D = 6.00 and 10.00 cm, the oil-saturated rock samples were suspended from a balance and immersed in distilled water. Change in the weight of the core as a function of time was monitored. The accuracy of the balance was 0.01 g, corresponding to an uncertainty of approximately ±0.02 mL of water imbibed. The mass of the rock samples was determined at the end of each run to check material balance; good agreement between measured volume and the weight of the rock sample was obtained in all tests.

All tests in part 2 of the experimental program were performed using the balance. The rock sample was suspended partly in water and oil (totally in water in two of the tests) from the balance, and change in weight was recorded as a function of time (Figure 4). At the end of each run, ultimate recovery was determined from difference in mass of the rock sample and the fluid densities. This value was used to calibrate the intermediate recorded masses on the imbibition curve to correct for the effect of the downward movement (approximately 0.6 cm) of the oil−water contact during each run (the movement will induce decreasing buoyancy forces).

Results and Discussion

A total of twenty-five SI tests have been performed to evaluate the impact of different rock sample shapes, sizes, and boundary conditions on the oil recovery rate. Out of these, fifteen tests were performed under counter-current flow conditions to compare predicted L_C values with experimental data varying the sample shapes (cylindrical, cubic and irregular shapes), sizes (diameter of cylindrical rock samples) and the boundary conditions (AFO, 2FC, etc.). The relationship between oil recovery and imbibition time for these fifteen tests are presented in Figure 5 (the results for the counter-current tests are presented using log-scales due to large variations in imbibition time).

The figure shows that counter-current SI rate is strongly dependent on geometry and boundary conditions. The time span between the fastest (Test 3) and the slowest (Test 13) test covered the range from 840 s (14 min) to approximately 60 000 s (≈16.5 h). Ultimate recoveries were usually close to 60% IOIP, but some tests approached 70% IOIP. The rock samples showing the highest recoveries were in general the tests having the slowest oil recovery rate. Furthermore, it should be noticed that all tests in this work were performed with initial water saturation (S_{wi}) equal to zero. Some variations in SI rate depending on S_{wi} have previously been observed. Viksund et al.[12] showed that the imbibition rate increased with increasing S_{wi} in the range 0−34% and decreased slightly for S_{wi} larger than 34% using strongly water-wet outcrop chalk material from Denmark. The variation either way was well within an order of magnitude. Small influence of S_{wi} was also observed when performing SI tests into preferential oil-wet chalk

(12) Viksund, B. G.; Morrow, N. R.; Ma, S.; Wang, W.; Graue, A. *SCA-paper 9814 presented at the Society of Core Analysts International Symposium*; Hague, The Netherlands, 1998.

Table 3. Core Data from SI Tests Performed in Part 2 of the Experimental Program

test no.	boundary condition (Oil (O); Water (W); Coated (C))	$V_b \times 10^{-6}$ (m^3)	PV $\times 10^{-6}$ (m^3)	Φ (%)	$A_{oil} \times 10^{-4}$ (m^2)	$A_{water} \times 10^{-4}$ (m^2)	$A_{coated} \times 10^{-4}$ (m^2)	WOAR
16	AFO	125	53.95	43.2	0	150		
17	O: Top surface; W: All other surfaces; C: −	125	54.50	43.6	25	125		5.00
18	O: Upper half; W: Lower half; C: −	125	54.55	43.6	75	75		1.00
19	O: Top and lateral surfaces; W: Bottom surface; C: −	125	54.38	43.5	125	25		0.20
20[a]	O: Top and lateral surfaces; W: Bottom surface; C: −	125	54.32	43.5	125	25		0.20
21	O: Upper half;W: Bottom surface; C: Lower half lateral surfaces	125	52.52	42.0	75	25	50	
22	O: Top surface; W: Bottom surface; C: All lateral surfaces	125	53.84	43.1	25	25	100	
23	O: −; W: One surface; C: 5 surfaces	125	53.68	42.9	0	25	125	
24	O: Top surface; W: Lower half; C: Upper half lateral surfaces	125	52.80	42.2	25	75	50	
25	O: 10% of top surface; W: Lower half; C: Upper lateral surfaces and 90% of top surface	125	52.20	41.8	2.5	75	72.5	

[a] Repeated Test 19.

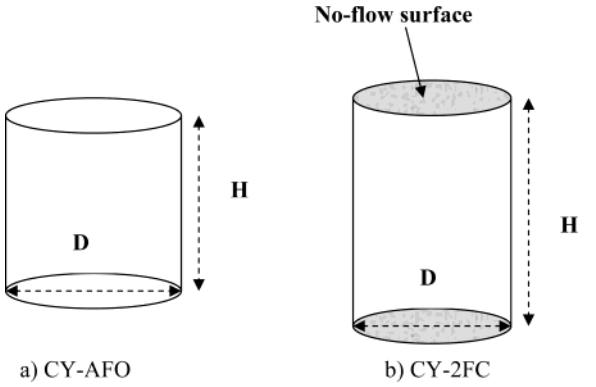

Figure 1. Cylinderical rock samples with diameter *D* and height *H*.

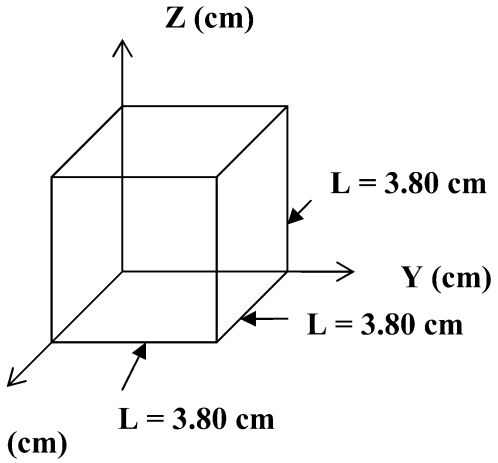

Figure 2. Boundary conditions for the cubic rock samples. The surfaces coated (NFS) were: CU-2FC ($X = Y = 0$), CU-4FC ($X = Y = Z = 0$, $Z = 3.80$ cm), CU-4FC (S) ($Y = Z = 0$, $Y = Z = 3.80$ cm), and CU-5FC ($Y = Z = 0$, $X = Y = Z = 3.80$ cm). The *Z*-axis was pointing upward in all tests.

material using surfactants[13] (imbibition time was typically 70% longer for cores with $S_{wi} \approx 25\%$ compared to cores without initial water saturation). The initial water saturation in low-permeability chalk reservoirs is usually low,[14] 5−10%, justifying the test condition used in this work. First, the results shown in Figure 5 will be discussed in the coming sections before discussing the SI curves for rock samples partly covered by an oil-phase (last 10 tests).

Calculated Characteristic Length for Cylindrical Rock Samples. Equation 2 for cylindrical cores (diameter *D* and height *H*) with all face opens (CY-AFO, Test 1) to imbibition yields for the L_C term: $L_C^2 = D^2H^2/4(D^2 + 2H^2)$. Here, $D = H$ (= 3.80 cm), and L_C^2 becomes equal to $D^2/12$. The SI process is 3-dimensional (3-D) counter-current, and the NFBs are the axis of the core and a circular plane through the center of the core, respectively. When the top and the bottom face are coated (CY-2FC, Tests 3−6), L_C^2 becomes $D^2/8$, i.e., L_C is independent of core height and determined by the diameter of the core sample. In this case, the NFB will be the axis of the core and the flow is 2-D radial counter-current. The calculated numerical values of L_C for cylindrical rock samples are given in Table 2.

SI into Cylindrical Core Samples. Five different rock samples having cylindrical shape were tested. One core had all faces open to fluid exchange, whereas four had the top and bottom face coated with polyester

(13) Standnes, D. C.; Austad, T. *J. Pet. Sci. Eng.* **2000**, *28*, 123−143.

(14) Spinler, E. A.; Hedges, J. H. *SCA paper presented at the International Symposium of the Society of Core Analysts*; San Francisco, CA, USA, 1993.

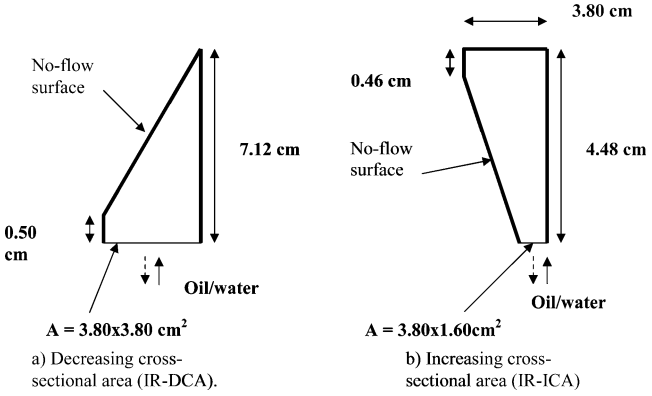

Figure 3. Boundary conditions for rock samples with varying cross-sectional area. Water (solid arrow), Oil (dashed arrow).

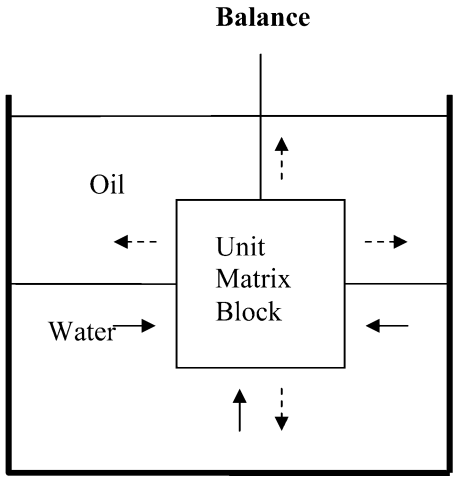

Figure 4. SI into a unit matrix block partly covered with oil and water (the WOAR = 1 in the case shown). Water (solid arrow), Oil (dashed arrow).

(creating NFS). The dimensionless time, $t_{D,MZM}$ is inversely proportional to L_C^2 and directly proportional to the real imbibition time (since C in eq 3 is essentially constant in all imbibition tests). Therefore, the L_C values predict the imbibition rate to decrease in the following sequence: CY-2FC (D = 1.99 cm) > CY-AFO ($H = D$ = 3.80 cm) > CY-2FC (D = 3.39 cm) > CY-2FC (D = 6.00 cm) > CY-2FC (D = 10.00 cm). The experimentally determined SI curves are depicted in Figure 6. The SI rate for the tests decreased in the order CY-2FC (D = 1.99 cm), CY-AFO ($H = D$ = 3.80 cm), CY-2FC (D = 3.39 cm), CY-2FC (D = 6.00 cm), CY-2FC (D = 10.00 cm), which is in qualitative line with the predicted calculated values. It is noticed that the two tests having the lowest imbibition rate CY-2FC (D = 10.00 cm) and CY-2FC (D = 6.00 cm) produced significantly more oil (≈70% IOIP) than the faster ones (≈60% IOIP). This can probably be related to the tendency for snap-off to decrease as the imbibition rate decreases.[15] Good reproducibility was obtained for the sample having all faces open to imbibition. The correctness of the relative oil recovery rates are confirmed quantitatively by plotting normalized oil recovery vs dimensionless time shown in Figure 7. All the SI curves fall approximately on one single line, confirming the ability for the L_C term to account for the different boundary conditions (AFO vs 2FC) and the variation in the diameter of the core samples (2−10 cm).

Calculated Characteristic Length for Cubic Rock Samples. For cubic rock samples with volume L^3 and all faces open (CU-AFO, Test 7) to imbibition, eq 2 yields $L_C^2 = L^2/12$. The NFBs are three perpendicular planes going through the center of the cube, and the flow is 3-D counter-current. The expressions for the other boundary conditions used are as follows: two faces coated (CU-2FC, Tests 8 and 9) → $L_C^2 = L^2/6$. The NFBs are the two coated faces (NFS) and a plane through the middle of the cube perpendicular to the coated surfaces. The flow is 3-D counter-current. Four faces closed for imbibition (CU-4FC, Test 10) → $L_C^2 = L^2/2$. The NFBs are the coated faces (NFS) opposite to the open surfaces. The flow is radial 2-D counter-current. Four faces coated (symmetric) → (CU-4FC(S), Test 11) → $L_C^2 = L^2/4$. The NFB is a square plane through the center of the rock sample. The flow is 1-D counter-current. Five faces coated (CU-5FC, Test 12) → $L_C^2 = L^2$. The NFB superimpose with the NFS opposite to the open surface and the flow is 1-D counter-current. Since all the cubes have equal size (L = 3.80 cm), the data predict for example the SI for the CU-AFO tests to be twelve times faster than the CU-5FC tests. The samples with four faces coated differ by a factor of 2 (CU-4FC and CU-4FC(S)). When the boundary condition allows imbibition from opposite surfaces (CU-4FC(S)), the imbibition rate should be one-half of the imbibition time for the sample having two neighboring faces open to fluid exchange (CU-4FC). Hence, it is not necessarily a direct proportion between imbibition rate and available area for water access. The geometry of the boundary conditions is also important regarding SI rates for rock samples having equal areas available for fluid exchange. Calculated numerical values for the L_C term for all cubic rock samples are given in Table 2.

SI into Cubic Rock Samples. Six tests were performed on rock samples having cubic shape (the CU-2FC test was repeated). The numerical L_C values predict the rate to decrease in the following order: CU-AFO, CU-2FC, CU-4FC(S), CU-4FC and CU-5FC. The results from the experimentally determined SI tests are depicted in Figure 8. The results show that the SI rates decreased in the order CU-AFO, CU-2FC ≈ CU-4FC-(S), CU-4FC and CU-5FC, which is in good agreement with the predicted rates (L_C-values) calculated from eq 2. Again, the test showing the slowest imbibition rate (CU-5FC) produced most oil (≈65% IOIP), whereas the faster tests ceased at about 60% IOIP as for the cylindrical samples. Higher tendency for snap-off of oil to occur for the faster test can again be the explanation for the difference in ultimate recovery. The sample having 2FC was tested twice, and good reproducibility was obtained again.

Scaled SI curves for the cubic rock samples are shown in Figure 9. The curves fit approximately into one single line showing that the L_C term is able to account properly for all the tested boundary conditions. A slightly slower oil recovery rate occurs for the CU-5FC sample as a function of dimensionless time.

SI into Cubic and Cylindrical Rock Samples with AFO. The L_C values in Table 4 indicate that the SI rate into cylindrical cores should be equal to the

(15) Schechter, D. S.; Zhou, D.; Orr, F. M., Jr. *J. Pet. Sci. Eng.* **1994**, *11*, 283−300.

Table 4. Predicted Characteristic Length Terms for Tests Performed on Cylindrical, Cubic, and Irregular Rock Samples in Part 1 of the Experimental Program

Characteristic Length L_C for Cylindrical Rock Samples

test no.	boundary condition	L_C^2	diameter (m)	height (m)	$L_C^2 \times 10^{-4}$ (m^2)
1	CY-AFO	$D^2/12$ ($D = H$)	0.0380	0.0380	1.2
2	CY-AFO (repeated test 1)	$D^2/12$ ($D = H$)	0.0380	0.0380	1.2
3	CY-2FC	$D^2/8$	0.0199	0.0500	0.5
4	CY-2FC	$D^2/8$	0.0339	0.0496	1.4
5	CY-2FC	$D^2/8$	0.0600	0.0320	4.5
6	CY-2FC	$D^2/8$	0.100	0.0397	12.5

Characteristic Length L_C for Cubic Rock Samples

test no.	boundary condition	L_C^2	length (m)	$L_C^2 \times 10^{-4}$ (m^2)
7	CU-AFO	$L^2/12$	0.0380	1.2
8	CU-2FC	$L^2/6$	0.0380	2.4
9	CU-2FC (repeated test 8)	$L^2/6$	0.0380	2.4
10	CU-4FC	$L^2/2$	0.0380	7.2
11	CU-4FC(S) (symmetric)	$L^2/4$	0.0380	3.6
12	CU-5FC	L^2	0.0380	14.4

Characteristic Length L_C for Irregular Rock Samples

test no.	boundary condition	L_C^2	imbibition area $\times 10^{-4}$ (m^2)	$V_b \times 10^{-6}$ (m^3)	height (m)	$L_C^2 \times 10^{-4}$ (m^2)
13	IR-DCA	$V_b \cdot l/A$	14.4	54.70	0.0712	27.1
14	IR−CCA	$(4/\pi)\cdot(L^4/D^2)$	4.08	54.30	0.0380	24.7
15	IR−ICA	$V_b \cdot l/A$	6.08	47.90	0.0448	35.3

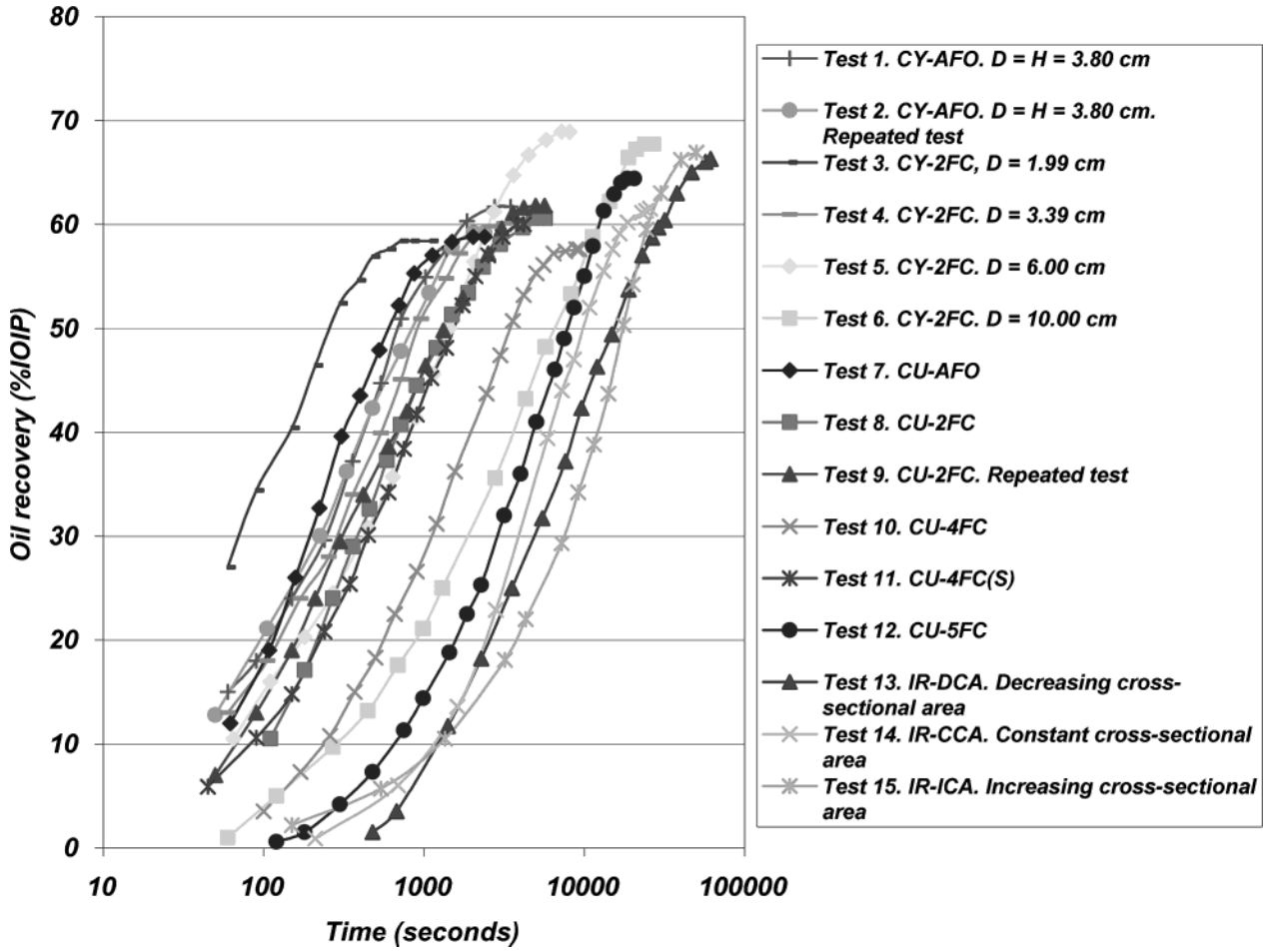

Figure 5. SI curves for all tests performed in part 1 of the experimental program varying sample shape, size, and boundary conditions.

imbibition rate into a cubic rock samples if the diameter (D) and height (H) of the cylindrical core is equal to the length of the side (L) of the cube. The imbibition curves shown in Figure 10 confirm the prediction as the two curves superimpose within the experimental error. Performing SI tests in the laboratory on cylindrical core samples having the height equal to the diameter is therefore representative for SI tests performed on cubic matrix blocks. The latter ones are probably closer to the shape of real reservoir matrix blocks. The similarity between Test 1 and Test 7 is also in accordance with the ratio between available area for imbibition and the

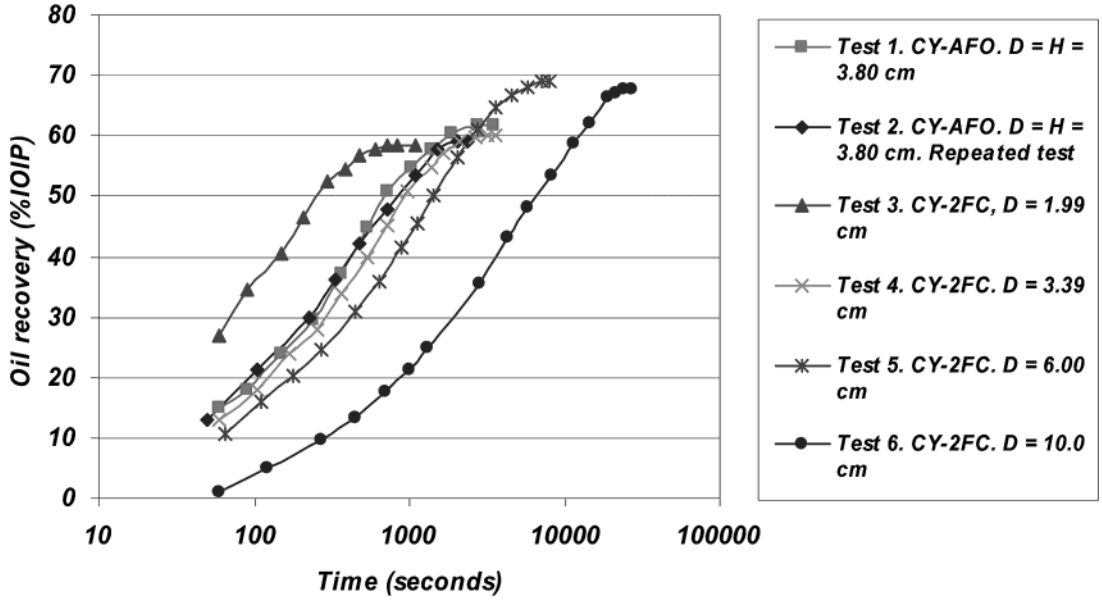

Figure 6. SI curves into cylindrical rock samples with different boundary conditions and sample sizes.

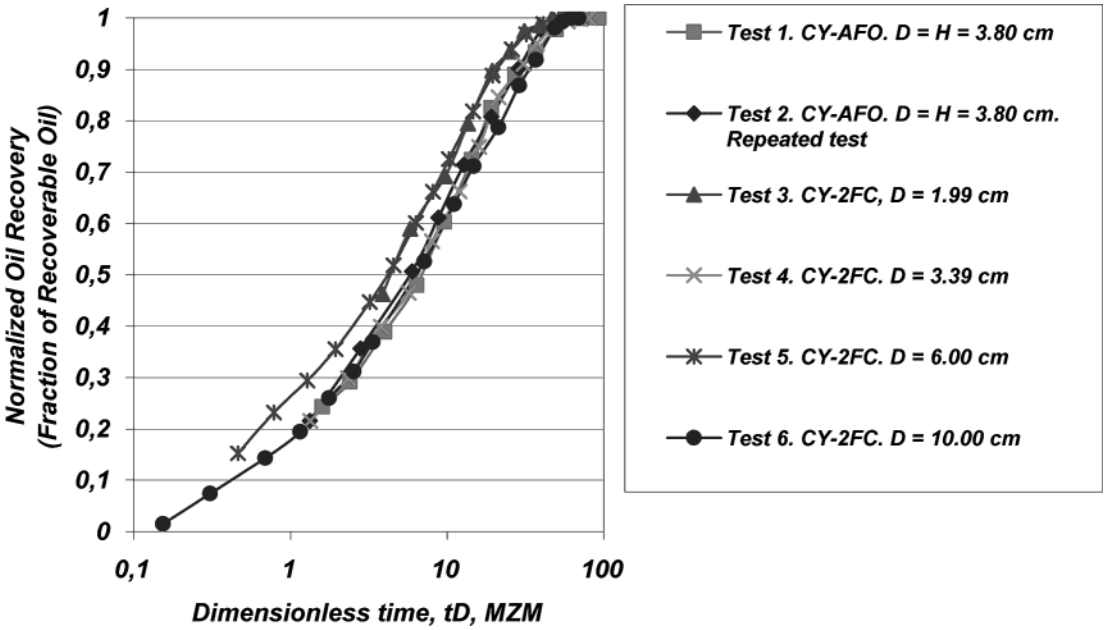

Figure 7. Normalized oil recovery vs dimensionless time, $t_{D,MZM}$ for cylindrical rock samples.

bulk-volume of the rock samples. If the length L of the sides in the cube equal the diameter and height of the cylinder, this ratio is equal to $(A/V)_{cube} = (A/V)_{cylinder} = 6/L$ for both geometries.

SI into Irregular Rock Samples/Boundary Condition. Three SI tests were performed on rock samples with irregular shapes/boundary condition. The IR-DCA sample (Test 13) had a decreasing cross-sectional area (DCA) and a total length of 7.12 cm (Figure 3a). The sample was laterally coated (NFS) and the only surface open to fluid exchange was a 3.80 cm × 3.80 cm square. The IR-CCA sample (Test 14) was cubic (constant cross-sectional area (CCA)) with all surfaces coated except a circular opening with diameter $D = 2.28$ cm. The origin of the circle was located in the middle of one of the surfaces. The IR-ICA sample (Test 15) had an increasing cross-sectional area (ICA) and a total length of 4.48 cm (Figure 3b). It was laterally coated with polyester, and the only face open to fluid exchange was rectangular with area 3.80 cm × 1.60 cm. The fluid flow in these three tests was 1-D counter-current, and oil recovery vs imbibition time is depicted in Figure 11. The two samples with the slowest initial rate recovered most oil, approximately 65% IOIP. Using the expression for the L_C term (eq 3) choosing the length from the face open to imbibition to the opposite end (total height of the rock sample) as the distance to the NFB gives L_C^2 equal to 24.7×10^{-4} m^2 for IR-CCA, 27.1×10^{-4} m^2 for IR-DCA, and 35.3×10^{-4} m^2 for IR-ICA, respectively, in line with early oil recovery rates (imbibition time is inversely proportionate to L_C^2). However, the oil recovery for the IR-ICA sample exceeded that from the IR-DCA sample after approximately 22 000 seconds. Hence, the overall shapes of the SI curves for the IR-DCA and IR-ICA differ from the curve generated by IR-CCA and they cannot be scaled to one single line only by multiplying with a constant. This is confirmed when plotting normalized oil recovery vs dimensionless time shown in

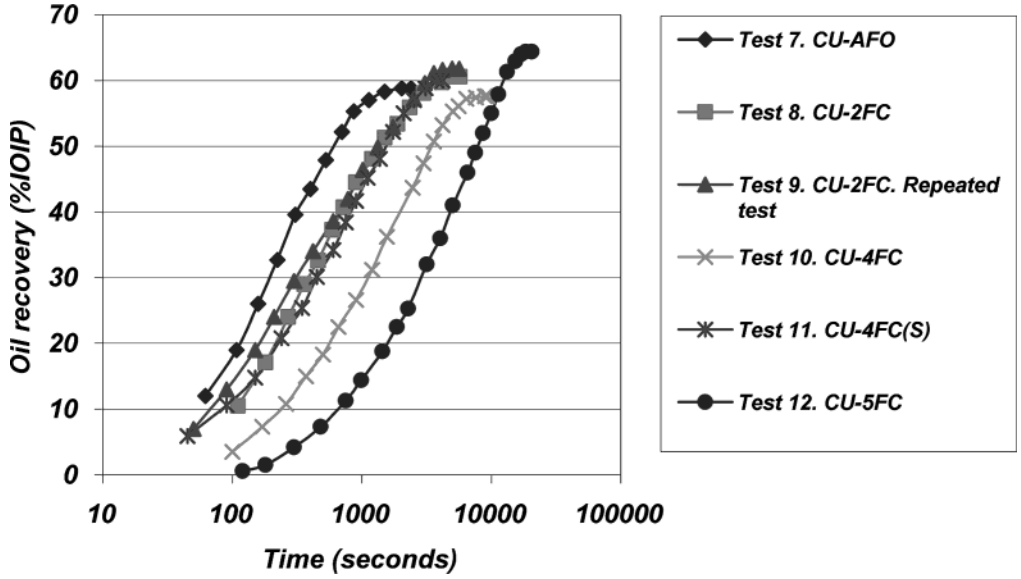

Figure 8. SI curves into cubic rock samples with different boundary conditions.

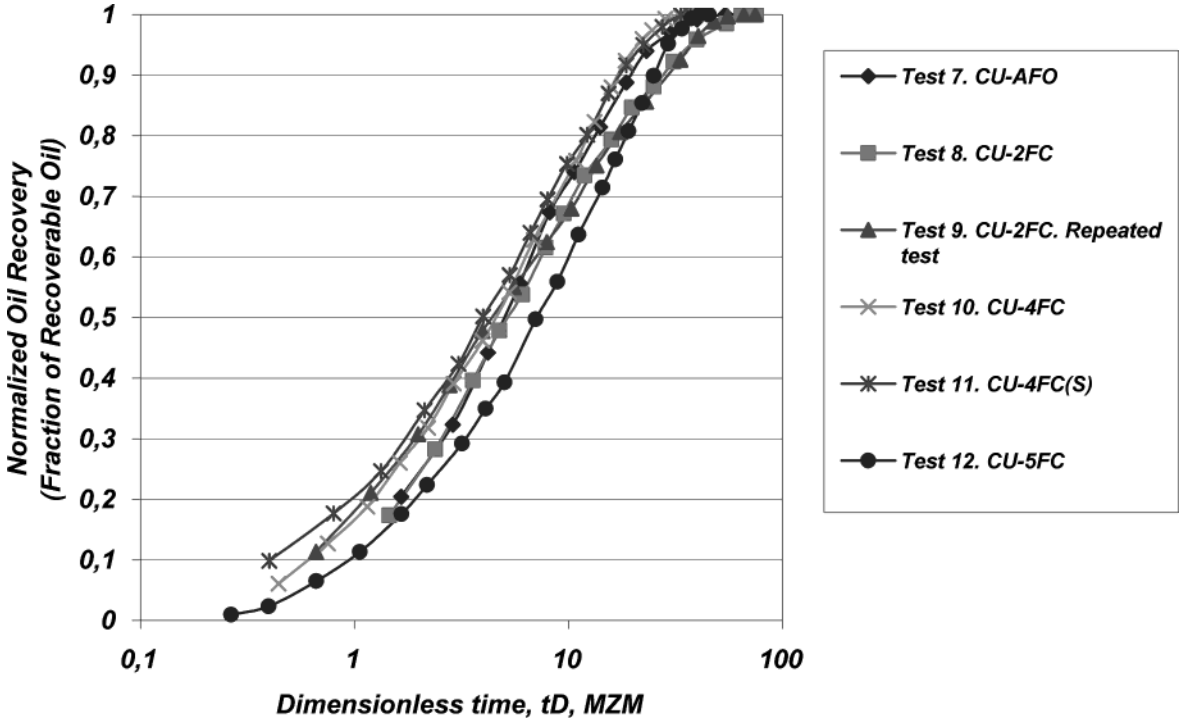

Figure 9. Normalized oil recovery vs dimensionless time, $t_{D,MZM}$ for cubic rock samples.

Figure 12. The curves cannot be scaled into a single line due to the difference in overall curve shape of the original SI curves in Figure 11. However, the shape of the imbibition curve for the IR-CCA sample resembles that of the curves generated by cylindrical and cubic rock samples, Figure 5. Hence, it looks like eq 2 is able to account for the reduction in fluid exchange area for the IR-CCA.

SI into Unit Matrix Block (UMB) Partly Covered by Oil. A total of ten SI tests were performed on a UMB with different boundary conditions (Figure 4 and Table 3). Eight of these were performed with both oil and water covering parts of the rock surface (co-current flow conditions), whereas two were performed with the cube totally submerged in water for the sake of comparison (counter-current flow conditions with boundary conditions AFO and 5FC). For the tests where only oil and water are covering the cube surface (i.e., no coating), it is convenient to define a water−oil area-ratio (WOAR) representing the ratio of the cube's area exposed to water to the area exposed to oil:

$$\mathrm{WOAR} = \frac{A_{\mathrm{water}}}{A_{\mathrm{oil}}} \tag{4}$$

where A_{water} represents the area of the cube covered by water (m^2), and A_{oil} is the area of the cube covered by oil (m^2).

Three different WOARs were applied in this study. WOAR = 5 when the cube was partly submerged in water and oil was covering the top surface. WOAR = 1 when half of the cube was exposed to water and the

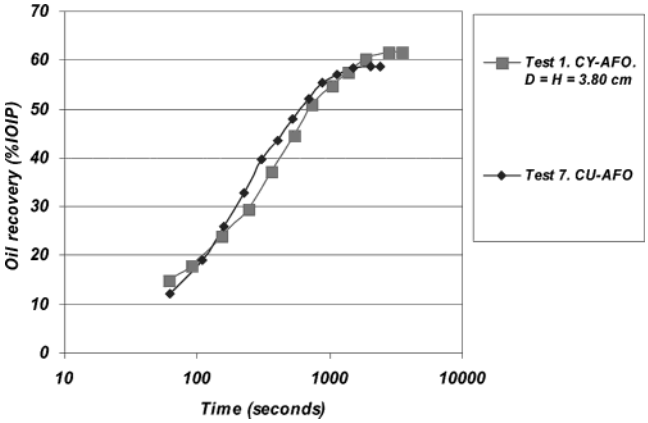

Figure 10. SI curves into cubic and cylindrical rock samples having all faces open to imbibition.

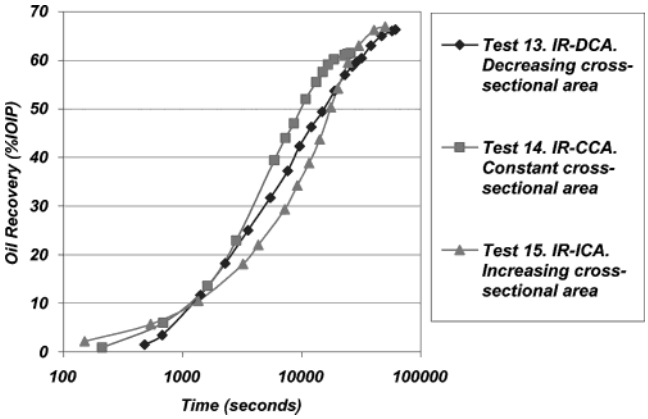

Figure 11. SI curves into rock samples with irregular geometry/boundary conditions.

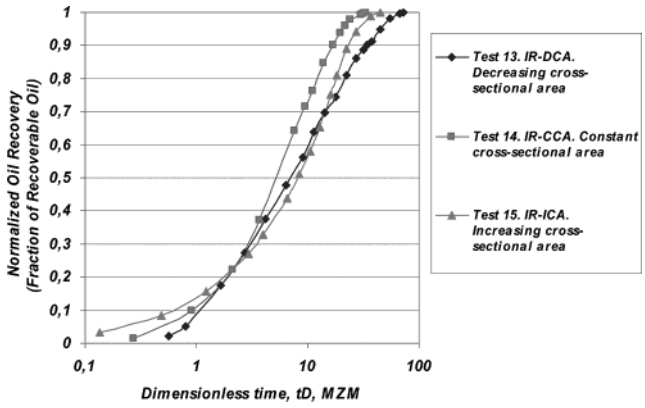

Figure 12. Normalized oil recovery vs dimensionless time for rock samples.

other half to oil, and finally WOAR = 0.2 when oil was covering all surfaces except the bottom face.

Figure 13 shows oil recovery vs imbibition time for all 10 tests performed in part 2 of the experimental program (linear scales are used for these tests due to much smaller variation in imbibition time). The depicted curves show that the co-current SI rate is strongly dependent on boundary condition. The time span for the tests performed under co-current flow conditions was in the range from 4600 (≈1 h and 17 min) for Test 17 to 34 000 seconds (≈9 h and 30 min) for Test 22. The maximum oil recovery level for all tests where oil covered part of the rock surface (co-current flow conditions) was significantly higher than for the tests where oil was produced counter-currently (Test 16 and 23). This is exemplified by the AFO test (Test 16) where maximum oil recovery ceased at 58% IOIP compared to 70−73% IOIP for the co-current tests. The tendency for snap-off of oil to occur therefore seems to be suppressed by co-current flow of oil and water compared to counter-current flow for comparable imbibition rates (Test 18 and 24). Tests performed under comparable conditions will be discussed in more detail in the next sections.

SI into UMB with Constant Oil Coverage. Variable areas available for water imbibition for constant coverage of oil (top surface and top half of the cube, respectively) are presented in Figures 14 and 15. It is very interesting to note in Figure 14 that co-current SI rate is higher when the top surface is exposed to oil (Test 17) compared to the case where all surfaces are open to water imbibition (Test 16 AFO, counter-current flow conditions). In the former case, the water imbibition area is reduced by 17% compared to the AFO case but the oil coverage on the top surface compensates and even accelerates the oil expulsion rate. The SI curve for Tests 22 and 24 show that the SI decreases significantly when the areas available for water imbibition decreases. The time to reach the plateau level for Test 22 was approximately 5 times longer than for Test 24 having only the upper half of the lateral surfaces covered with polyester, which again used approximately 50% longer time than Test 17 (only the top surface covered by oil) to reach the maximum oil recovery level. Thus, the lateral water availability is very important to maintain high oil recovery rates.

The same qualitative trend as in the previous figure is also seen for oil coverage of 50% depicted in Figure 15. Water had access to the bottom half in Test 18 (WOAR = 1) and the bottom-face only in Test 21. Again, the rate decreased when the lateral faces were nonaccessible for water imbibition. It is also interesting to note that 50% coverage of oil and water seems to be the critical WOAR distinguishing normalized oil recovery rates which are either higher or lower than the oil recovery rate generated under pure counter-current SI conditions (AFO). If the WOAR > 1, i.e., the oil−water contact is above the lower half of the cube, the oil recovery rate will be higher than compared to the AFO case and vice versa for WOAR below 1.

SI into UMB with Constant Water Coverage. The SI rate is much less sensitive for variable oil coverage than variable water availability. This is clearly demonstrated in Figure 16. All these tests have the lower half of the cube exposed to water. The SI rate is approximately the same regardless of whether the cube has the upper half covered by oil (WOAR = 1) or the upper half laterally coated with polyester (only top surface exposed to oil). Exposing the upper half of the cube laterally to oil does not seem to have any effect on the oil expulsion rate in this case. Test 25 had the upper half of the cube coated with polyester and only a circular opening on the top surface (D = 1.76 cm) was exposed to oil (the circle covered an area approximately equal to 10% of the top-face area). A decrease in the oil recovery rate was observed, but the rate did not change very much relative to Test 18 having the whole upper half of the cube exposed to oil. It seems that water

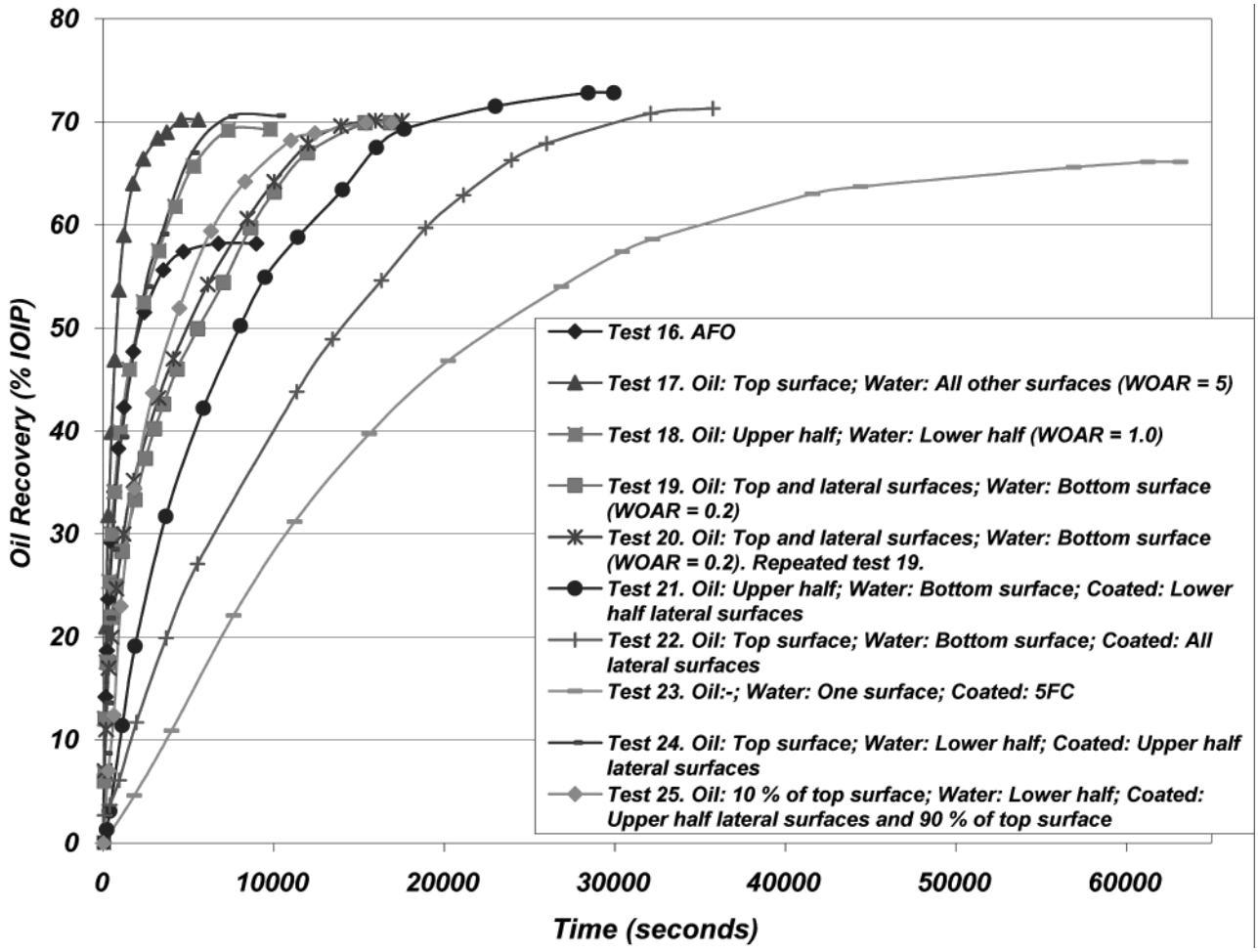

Figure 13. SI curves into unit matrix block with different boundary conditions (part 2 of the experimental program).

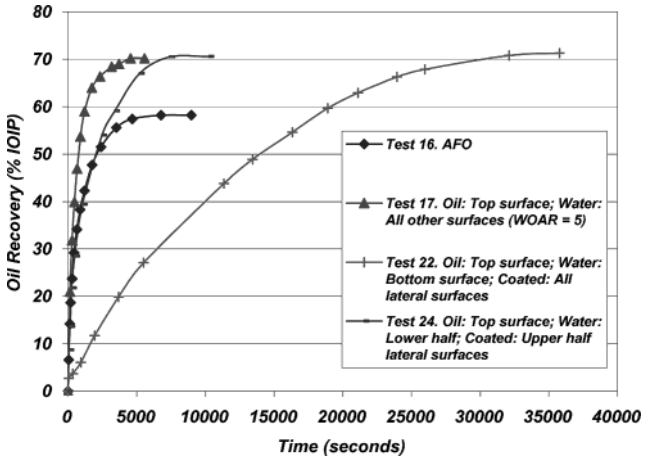

Figure 14. SI into UMB with area exposed to oil constant (top surface of the cube). Variation in the area exposed to water.

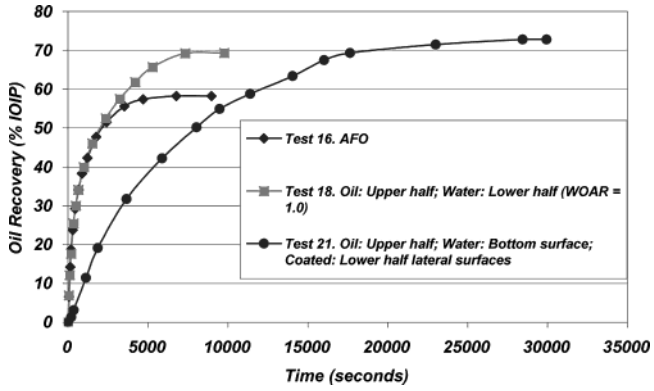

Figure 15. SI into UMB with area exposed to oil constant (upper half of the cube). Variation in the area exposed to water.

imbibition can be enhanced if some portion of the rock surface is exposed to oil, even though very small. However, when water only had access to the bottom-face, variable oil coverage comes into play. There is a small increase in the SI rates with increasing oil coverage as can be seen in Figure 17, but the differences are much smaller than for the case when the top surface was exposed to an oil-phase and the area available for water imbibition varied (Figure 14).

1-D Co-Current and 1-D Counter-Current SI. Oil recovery due to 1-D co-current and 1-D counter-current SI are compared in Figure 18. The cube was laterally coated with polyester, water imbibed from the bottom-surface against gravity and oil was covering the top surface in the co-current flow tests (Test 22). It was observed qualitatively that almost all the oil was produced co-currently and counter-current back-flow production was estimated to constitute approximately 5−10% of the total production of oil. This oil was produced quickly after initiating the imbibition test. These observations are in qualitative line with modeling results reported by Pooladi-Darvish and Firoozabadi.[9]

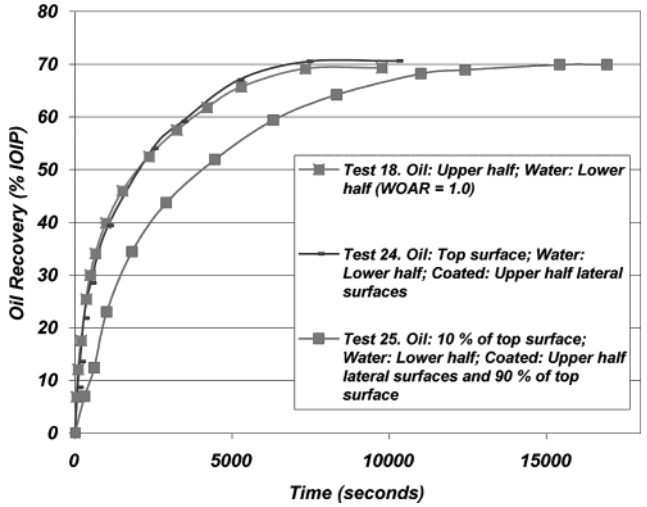

Figure 16. SI into UMB with area exposed to water constant (lower half of the cube). Variation in the area exposed to oil.

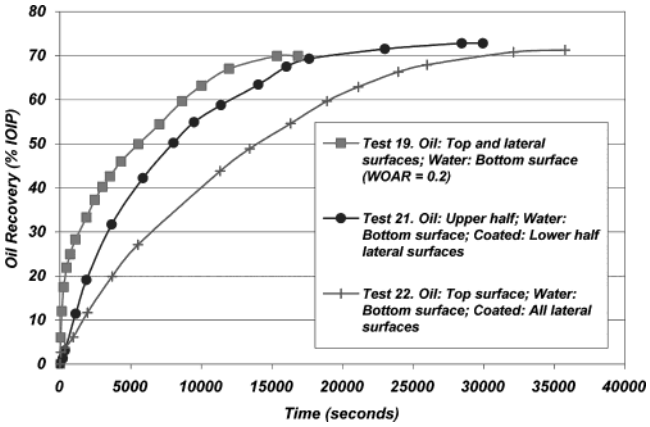

Figure 17. SI into UMB with area exposed to water constant (bottom face of the cube). Variation in the area exposed to oil.

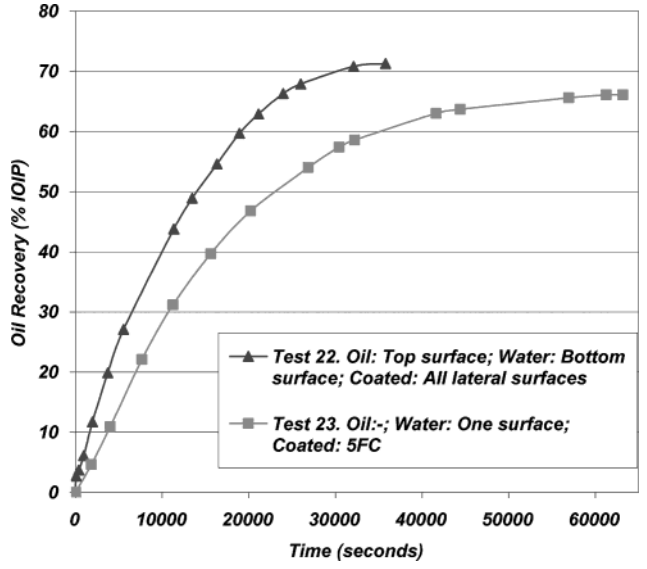

Figure 18. Comparison between 1-D counter-current and 1-D co-current flow of oil and water.

They found that the back production due to counter-current flow of oil and water represented approximately 5% of recoverable oil and was almost insensitive to core length. The counter-current flow test was performed by coating 5 faces of the cube with polyester and the face open to fluid exchange pointed downward during the test (water was therefore imbibing against gravity also in this case). The results show that co-current SI is faster than counter-current imbibition, approximately half the time to reach the plateau level, and ultimate oil recovery is higher (71% IOIP vs 67% for the counter-current case). This is comparable to the half time recoveries of 7.1 and 22.2 h observed by Bourbiaux and Kalaydjian[10] for co-current and counter-current SI, respectively. It should be mentioned that their data were obtained using medium permeability sandstone (≈130 mD) from the Vosges region in France, whereas low-permeability chalk was applied in this work.

General Comments. Comparison of oil recovery rates vs recovery rates generated under counter-current flow conditions (AFO) is of special interest because the latter ones are usually used when predicting potential oil recovery rates due to SI. The curve for Test 17 in Figure 14 as compared to Test 16 in the same figure indicates that evaluating the SI potential under counter-current test conditions may under certain circumstances lead to pessimistic forecasts regarding both oil recovery rates and ultimate recoveries. The results presented here may have applicability regarding the oil recovery mechanism in low-permeability fractured reservoirs such as the Ekofisk field in the North Sea. The reservoir rock in Ekofisk is strongly water-wet low-permeable fractured chalk similar to the outcrop material used in this study. Water injection was initiated in 1987 with great success and counter-current SI was assumed to be an important driving mechanism. The field performance due to water injection even exceeded expectations based on results obtained in laboratory tests.[16] The tests performed under co-current flow conditions in this work indicate the possibility that also this flow mode might contribute to the highly efficient SI process taking place in the Ekofisk field.

Conclusions

The results show that oil recovery induced by counter-current and co-current SI is highly dependent on sample shape, size (cylindrical cores) and boundary conditions. The following conclusions can be drawn from this work:

(i) The characteristic length term, L_C, is able to account quantitatively for differences in rock sample shape (cubic and cylindrical samples have been used), size (diameters in the range 2−10 cm for cylindrical cores) and boundary conditions (2, 4 and 5 FC for cubic rock samples; top and bottom faces closed for cylindrical samples).

(ii) L_C is not able to account properly for irregular sample shapes (increasing and decreasing cross-sectional imbibition areas were investigated) due to an overall difference in the shape of the imbibition curves.

(iii) Co-current flow of oil and water may, depending on the WOAR value, imply faster (WOAR > 1), equal (WOAR ≈ 1), or slower (WOAR < 1) oil recovery than SI into the unit matrix block having all faces open to imbibition (counter-current flow conditions). In all tests, ultimate recovery was significantly higher for the tests performed under co-current conditions than under counter-current flow conditions, 70−73% IOIP vs ≈58% IOIP.

(16) Hallenbeck, L. D.; Sylte, J. E.; Ebbs, D. J.; Thomas, L. K. *SPE FE* **1990**, *September*, 284−295.

(iv) When evaluating the oil recovery potential on reservoir rock samples by SI experimentally, tests should be performed under both co-current and counter-current flow conditions as the latter may under certain circumstances predict too low rates and ultimate recoveries

Acknowledgment. The author thanks Norsk Hydro for providing the chalk material used in this study, Steinar Vatne and Jozef Kusior at the University of Bergen for manufacturing the different rock sample geometries, Dr. Morten Gunnar Aarra and Ph.D. student Skule Strand for support during experimental work, and Prof. Arne Skauge for valuable discussions.

Nomenclature

A = area (m^2)
A_{coated} = area of cube covered by polyester (m^2)
A_i = area of ith imbibition surface (m^2)
A_{oil} = area of cube covered by oil (m^2)
A_{water} = area of cube covered by water (m^2)
AFO = all faces open
C = coated
C = constant (= 3.2×10^{-6} m^2/s)
CCA = constant cross-sectional area
CU = cubic rock sample
CY = cylindrical rock sample
D = diameter (m)
DCA = decreasing cross-sectional area
# FC = number of faces coated with polyester
H = height (m)
ICA = increasing cross-sectional area
IFT = interfacial tension (N/m)
IOIP = initially oil in place (m^3)
IR = rock sample having either irregular shape or boundary condition
k = absolute permeability (m^2, mD)
l_i = distance from ith imbibition surface to the no-flow boundary (m)
L = length of rock sample (m)
L_C = characteristic length (m)
$L_{C,MK}$ = characteristic length (Mattax-Kyte) (m)
NFB = no flow boundary
NFS = no flow surface
O = oil
PV = pore volume (m^3)
S = symmetric
S_{wi} = initial water saturation (% of pore volume)
SI = spontaneous imbibition
t = imbibition time (s)
$t_{D,MK}$ = dimensionless time (−) (Mattax-Kyte)
$t_{D,MZM}$ = dimensionless time (−) (Ma-Zhang-Morrow)
UMB = unit matrix block ($5.0 \times 5.0 \times 5.0 \times 10^{-6}$ m^3 cube)
V = volume (m^3)
V_b = bulk volume (m^3)
W = water
WOAR = water−oil area-ratio (m^2/m^2)
1-D = 1-dimensional
2-D = 2-dimensional
3-D = 3-dimensional
Φ = porosity (fraction or percentage of bulk volume)
μ_g = geometrical mean of water and oil viscosity (Pa·s)
μ_o = oil viscosity (Pa·s)
μ_w = water viscosity (Pa·s)
σ = oil−water IFT (N/m)

EF030142P